Contribution 14

Probing New Physics with Single Top + X

Devin G. E. Walker, Jiang-Hao Yu and C.-P. Yuan

Abstract
We investigate single top production in association with a variety of Standard Model final states with a focus on the early LHC run. Here X can be jets, large missing transverse momentum and/or electroweak gauge bosons. For this review, we focus on searches for new W' gauge bosons and heavy B' quarks. A general survey of the possible new physics with associated single top production can be found in Ref. [401]. In essence, the channel probes a variety of new physics, is intricately tied to the new physics at the TeV scale and is essential for maximizing the potential of the early LHC for new physics.

1 Introduction

For the first time in history, the TeV scale is being directly probed by the CERN Large Hadron Collider (LHC). Even at this early stage, hints of the Standard Model (SM) higgs boson [144, 402] as well as strong constraints on new physics have been produced. Of particular interest are the constraints on new scalar and gauge bosons (e.g. resonances [403–411]) as well as new exotic fermions [371, 412, 413] which are harbingers of natural new physics scenarios. Some of the most popular scenarios which exhibit this new physics can be found in Refs. [304, 306, 316, 381, 414–425]. In this review, we show how associated single top production (a top quark produced in conjunction with a variety of SM final states) can provide a sensitive probe to heavy B' quarks and W' gauge bosons.

A Motivation from Top Collider Physics: The LHC is a "top factory." At 7 TeV, 85,000 single top quark events are expected for 1 fb^{-1} of data [426]. Importantly, the production cross section for these background SM events are precisely known at next-to-leading order (NLO) and next-to-leading log (NLL). In addition, processes involving single top (quark) production may be unique in their ability to probe the nature of electroweak symmetry breaking. The top quark mass is of order the electroweak scale thereby suggesting that top quark production may be sensitive to new physics beyond the SM. Unlike other quarks, SM top quarks decay to a W boson and a bottom quark *before* hadronizing. This provides a unique opportunity to probe the underlying electroweak interactions as well as efficiently tag the events. Observation of SM single top production has been experimentally challenging. One of the major reasons is the jet not associated with the top decay is frequently in the forward regions in the detector. It is therefore hard to distinguish these single top events from the dominant QCD backgrounds. The fact that SM single top production has this difficulty is a ***strength*** when considering single top production from new physics. When new physics is produced that decays to single top $+X$, the large mass of the new physics often results in the decay products being in the center of the detector.

This review paper is organized as follows: In the next section, we outline the new physics that can be produced from single top $+X$ production at the LHC. As mentioned in the abstract, we restrict our focus to new W' bosons as well as new heavy quarks in this review. Please see Ref. [401] for an analysis of all the new physics listed in the next section. Appendix A includes a brief overview of our reconstruction methodology and any important definitions. Sections 3, 4 and 5 contain our analysis for the new W's and heavy quarks. Finally we conclude.

2 New Physics Searches with Single Top + X

This review is part of a larger series of papers searching for new physics in the single top + X final state [401]. Here we list the new physics that can be probed.

Single Top Signatures (partonic level)	New Physics Probed
$t + b$-jet/jet	W' Gauge Bosons Diquark Resonances Colored Resonances Charged Higgses
$t + Z/W$ (+ jet)	Heavy Top Quarks Heavy Bottom Quarks
$t + h +$ jet/W	SM Higgs
$t + h^- + b$-jet	Charged Higgses
$t + W +$ jet	Charged $5/3$ Quarks
$t + \not{E}_T +$ jet	Dark Matter Top Fermion Partners (e.g. stops)

The above chart is constructed by considering all possible SM particles on the external legs. Based on the SM symmetries, all possible new physics in the intermediate state(s) are enumerated at tree-level with the simplest tree-level topologies. We require at least one SM top quark in the final state; and, the initial states are light quarks or gluons. For this review, we focus on W' bosons and heavy quarks.

3 Searching for W' Bosons with $t + b$-jet/jet

3.1 Theoretical Considerations for W' Bosons

Previous studies of W' bosons decaying to top quarks have focused on the LHC at center of mass energies of 14 TeV [427]. We examine the potential of the early LHC to identify W'

bosons during the early LHC as well as the experimental reach. Many natural models of new physics beyond the SM have relatively light W' bosons. They are needed to cancel quadratic divergences induced by SM W bosons on the higgs potential. However, the tightest exclusion limits come from leptophobic W' bosons which decay to dijets [407, 428]

$$280 < m_{W'} < 1500 \text{ GeV}. \tag{1}$$

To ensure a model independent analysis, we write down the following parametrization

$$\mathcal{L} = \frac{i\, g_2}{\sqrt{2}}\ \bar{q}_i \gamma^\mu (f_L P_L + f_R P_R)\, V_{ij}\ q'_j\ W'^{+}_{\mu} + \text{h.c.}, \tag{2}$$

where q and q' are the up and down-type quarks, respectively. Here $i = u, c, t$, $j = d, s, b$, and $g_2 = e/\sin\theta_W$. Also, V_{ij} is the Cabibbo-Kobayashi-Maskawa matrix and $P_{L,R}$ are the chirality projection matrices. For simplicity in the next section, we consider only the case with a purely left-handed current ($f_L = 1$, and $f_R = 0$); our study can be extended easily to other cases.

3.2 Signal and Background Processes for W' Searches

The s- and t-channel signal processes are

$$p\,p \to t\,\bar{b} + \text{h.c.} \qquad\qquad p\,p \to t\,q \quad \text{or} \quad \to \bar{t}\,q. \tag{3}$$

For the t-channel processes on the right, the t and $\bar{t}$ final states are equally possible because the initial b and $\bar{b}$ partons occur with equal probability. For this channel, we only consider top quarks that decay semi-leptonically. The isolated lepton (with a sufficiently large p_T) allows for the event to be effectively tagged. The following SM backgrounds are dominant:

$$p\,p \to t + \text{jet(s)} \qquad\qquad p\,p \to W + \text{jets} \tag{4}$$

$$p\,p \to \bar{t}\,t \qquad\qquad p\,p \to W\,W/Z \tag{5}$$

The SM $p\,p \to t + \text{jet(s)}$ background is irreducible. The other SM backgrounds in equations 4 and 5 are important insofar as they can mimic the $t + \text{jet}$ final state.

3.3 Event Simulations for W' Searches

We focus on a 1.5 TeV W' boson with coupling $f_L = 1$. (See equation 2.) We use CTEQ6L parton distribution functions [429] in our event simulations. The renormalization and factorization scales are chosen to be the W' boson mass. The signal and background events are generated with MadGraph5/MadEvent. We impose the following basic p_T cuts

$$p_T^j \geq 25\,\text{GeV} \qquad\qquad p_T^\ell \geq 25\,\text{GeV}. \tag{6}$$

We also confine our search to the center of the detector

$$|\eta_j| \leq 2.5 \qquad\qquad |\eta_\ell| \leq 2.5. \tag{7}$$

As mentioned in the introduction for SM single top production, the jet not associated with the top quark decay is often forward in the detector. Restricting our focus to the center of the detector helps to eliminate this background. As mentioned before, we also require the leptons and jets to be well separated. We require the following cone sizes

$$\Delta R_{jj} > 0.4 \qquad\qquad \Delta R_{j\ell} > 0.4 \qquad\qquad \Delta R_{\ell\ell} > 0.2. \tag{8}$$

Since we require the top quark to decay semi-leptonically, the resulting neutrino introduces missing transverse momentum ($\not{E}_T$) in the event. To further reduce the SM background, we require

$$\not{E}_T > 25 \text{ GeV}. \tag{9}$$

The $t + \text{jet}$ signature has a final state with one isolated charged lepton (electron or muon), two high p_T jets, and large missing transverse momentum ($\not{E}_T$) from the missing neutrino. Large p_T cuts on the leading jet can be used to suppress most of the backgrounds. In the upper panels of Figure 1, we show the p_T distributions for the leading and sub-leading jets for the signal and background. As reminder, we consider the 1.5 TeV W' boson with $f_L = 1$ as the signal; the discriminating power of the p_T cuts is clear in those plots. We require

$$p_T \geq 200 \text{ GeV} \quad (\text{leading jet}), \tag{10}$$

$$p_T \geq 80 \text{ GeV} \quad (\text{subleading jet}). \tag{11}$$

Another useful variable is the scalar sum of the p_T's of all the particles in the final state. In Appendix A, we define

$$H_T = p_T^{\ell^+} + \not{E}_T + \sum_j p_T^j. \tag{12}$$

Here j runs over all of the well-separated jets in the event. We apply the following cut

$$H_T \geq 600 \text{ GeV}. \tag{13}$$

In Figure 1, a slight signal is visible near 1.5 TeV. To further optimize the signal, we apply b-tagging and perform standard sideband analysis. We apply the following invariant mass window cut

$$|m_{l\nu jj} - M_{W'}| < 400 \text{ GeV}. \tag{14}$$

Here $M_{W'}$ center of the resonance peak in the invariant mass distribution in Figure 1. Of course, the ν momentum is determined with the top reconstruction in Appendix A. After all of the cuts, a 1.5 TeV W' boson with a coupling of $f_L = 1$ is clearly visible. For reference, after all of the cuts, the s-channel and t-channel signal cross sections are

$$\sigma(p\,p \to W' \to b\,l^\pm\,\nu\,\bar{b}) = 13.136 \pm 0.0246 \text{ pb}, \tag{15}$$

$$\sigma(p\,p \to t(\bar{t})\,q \to b(\bar{b})\,l^\pm\,\nu\,q) = 8.5404 \pm 0.0218 \text{ fb}. \tag{16}$$

Table 1 gives a breakdown of the effect of the cuts on the signal and background cross sections.

3.4 Discovery Potential and Chiral Properties for W' Boson Searches

The SM backgrounds are suppressed efficiently such that less than 1 background event survives after cuts with an integrated luminosity of 10 fb $^{-1}$. We now consider a 1 GeV W' gauge bosons with $f_L = 1$. For that amount of luminosity we achieve

$$S/\sqrt{B} \sim 5 \tag{17}$$

where S and B denotes the number of signal and background events, respectively.

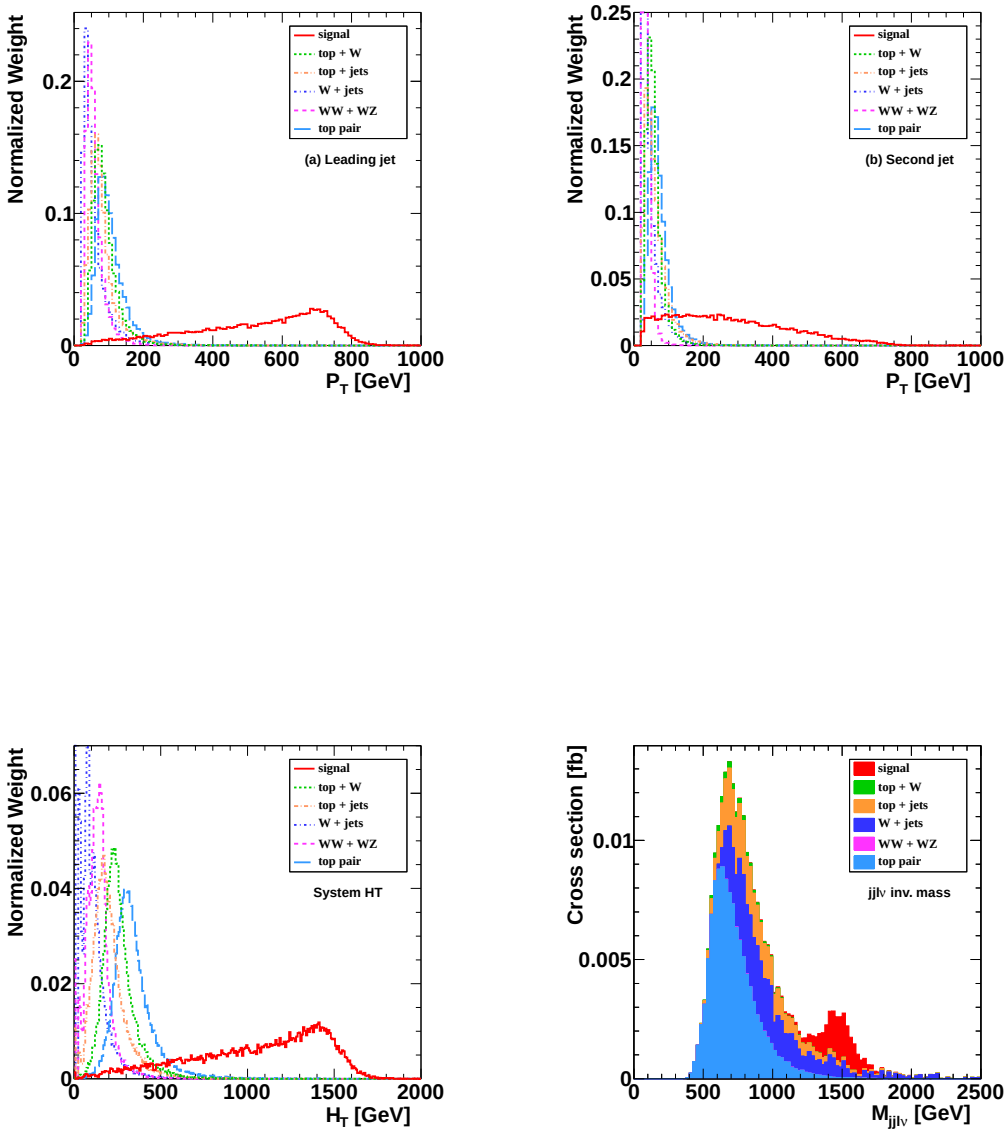

Figure 1: Normalized p_T distributions of the leading jet (upper left panel) and sub-leading jet (upper right panel) for the signal and backgrounds. The signal process features a 1.5 TeV W' boson with the coupling $f_L = 1$. See equation 2 for the definition of f_L. The H_T distributions for signal and backgrounds are also plotted (lower left panel). It is clear an H_T cut can be useful in separating the signal and backgrounds. After the cuts in equations 6-11 and equation 13 are made, the invariant mass distribution is plotted (lower right panel).

σ(fb)	Signal	$t+W$	$t+$jets	$t\bar{t}$	WV	$W+$jets
No cuts	58.96	2861	18877	25840	9888	4018600
Basic cuts (in eq. 6-9)	33.38	833	4049	7207	2265	284516
+ hard p_T cuts (in eq. 10-11)	28.65	11.1	158.5	232.6	3.67	7836.2
+ H_T cut (in eq. 13)	26.45	5.69	59.8	137.6	3.51	3782
+ Tagged b-jet	22.36	3.44	44.8	115.7	0.19	61.98
+ Mass window (in eq. 14)	21.59	0.13	7.80	3.97	0.03	16.02

Table 1: Cross sections for the signal and various background processes without and with the cuts are listed.

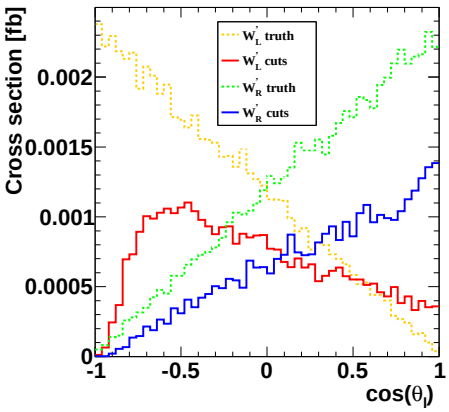

Figure 2: The angular distributions of the final lepton $\cos\theta_l$ for the left-handed W'. See Appendix A for definitions of $\cos\theta_l$.

After the discovery of the W' boson, one would like to know its mass, spin, and couplings. Angular distributions of its decay products can be investigated to definitively determine the spin and chiral structure of the W' boson to the SM fermions. The chirality of the W' coupling to SM fermions is best measured from the polarization of the top quark. Among the top quark decay products, the charged lepton from $t \to b + l + \nu$ is the best analyzer of the top quark spin. For a left-handed top quark, the charged lepton moves preferentially against the direction of motion of the top quark, while for a right-handed top quark the charged lepton moves along the direction of motion of the top quark. The angular correlation of the lepton is $(1 \pm \cos\theta_l)/2$, with the $(+)$ choice for right-handed and $(-)$ for left-handed top quarks, where θ_l is the angle of the lepton in the rest frame of top quark relative to the top quark direction of motion in the center-of-mass (c.m.) frame of the incoming partons. In Figure 2, we plot $\cos\theta_l$ for $f_L = 1$,

$f_R = 0$ (W'_L) as well as $f_L = 0$ and$f_R = 1$ (W'_R). We expect a flat angular distribution for the SM $t\bar{t}$ background because the top quark and anti-top quark are not polarized. Therefore, the angular distributions of the lepton can be used to discriminate W' models in which the chirality of the W' coupling to SM fermions differs.

4 Searching for Heavy Top and Bottom Quarks with $t + W +$ jet

4.1 Theoretical Considerations for Heavy Quarks

In many models of natural electroweak symmetry breaking, the following tree-level coupling exists

$$B' \to W\, t \tag{18}$$

with $\mathcal{O}(1)$ strength. Often the heavy bottom quarks are vector-like because of the minimal impact on precision electroweak bounds. In natural theories, heavy top partners (and the corresponding bottom partners) are *essential* for canceling the quadratic divergences induced by the SM top quark on the higgs potential. Thus, these particles are expected to be relatively light. Recent experimental bounds on heavy tops and bottom quarks are [430]

$$m_{T'} \geq 311 \text{ GeV}, \qquad\qquad m_{B'} \geq 338 \text{ GeV}\,. \tag{19}$$

We show this bound can be improved during the early LHC running. In this review, we restrict our focus to B' heavy quarks production with a $t + W$ final state. We parameterize the heavy quark interactions in a manner similar to Ref. [431] in order to keep our analysis model independent[1]. After electroweak symmetry breaking, the effective couplings between the electroweak gauge bosons, the third generation SM quarks and the new heavy quarks is

$$\begin{aligned}\mathcal{L} &= \frac{g_2}{\sqrt{2}}\, W^+_\mu \left(\bar{t}\,\gamma^\mu (f^L_{tB'} P_L + f^R_{tB'} P_R) B' \right) + \frac{g_2}{\sqrt{2}}\, W^-_\mu \left(\bar{b}\,\gamma^\mu (f^L_{bT'} P_L + f^R_{bT'} P_R) T' \right) \\ &+ \frac{g_2}{2\, c_W} Z_\mu \left(\bar{t}\,\gamma^\mu (f^L_{tT'} P_L + f^R_{tT'} P_R) T' + \bar{b}\,\gamma^\mu (f^L_{bB'} P_L + f^R_{bB'} P_R) B' \right) + h.c. \end{aligned} \tag{20}$$

Here g_2 is the $SU(2)_L$ coupling, c_W is the cosine of the Weinberg angle, $P_{L,R}$ are the usual projection operators and f parametrizes the chirality of the couplings. For the vector-like heavy quarks, the couplings $f_{qQ'}$ in the above Lagrangian can be parametrized in a model independent way as

$$f^{L,R}_{qQ'} \simeq \frac{v}{m_{Q'}} \kappa^{L,R}_{qQ'}\,, \tag{21}$$

where $\kappa^{L,R}_{qQ'}$ is a dimensionless parameter. For the chiral heavy quarks, the couplings f_{qQ} are equal to

$$f^L_{qQ'} = \left| V^{CKM}_{qQ'} \right|\,, \quad f^L_{qQ'} = 0\,. \tag{22}$$

In order to generate the heavy bottom quark resonance, we require the following magnetic moment operator

$$\mathcal{O}_1 = \frac{g_s\, \lambda_i^2}{2 M_{B'}}\, \overline{B'}\, \sigma^{\mu\nu}\, G_{\mu\nu}\, b, \tag{23}$$

[1] In Ref. [431], the new heavy quarks couple preferentially to first generation quarks. Thus, the decay of the heavy quarks will involve light quarks instead of the top.

σ(fb)	Signal	$t+W$	$t+\text{jets}$	$t\bar{t}$	$WV+\text{jets}$	$W+\text{jets}$
No cuts	681.570	2861.00	18877.0	22200.0	10007	2457400
Basic cuts	326.199	833.695	4049.12	5575.53	1721.2	88343.5
+hard cuts	210.469	151.776	257.671	2888.22	288.202	23713.9
+HT cuts (in Eq. 31)	196.531	52.3563	90.6096	1247.64	125.087	12901.4
+Tagging one b-jet	118.559	33.4737	46.2486	580.530	32.5228	284.724
+Mass window cuts in Eq.33	98.4187	12.7315	17.9331	147.630	10.0070	81.3498

Table 2: Cross sections for the signal and various background processes without and with the cuts are listed.

where $G_{\mu\nu} = G^a\,T^a/2$ is the field strength tensor of the gluon and g_s is the strong coupling constant. By naive dimensional analysis, we take the suppression scale to be twice the excited resonance mass.

4.2 Signal and Background Processes for Heavy Bottom Quarks

As alluded to above, for heavy bottom quarks the signal production processes are

$$p\,p \to B' \to t\,W^- \tag{24}$$

with the final decays

$$W^\pm \to l^\pm\,\nu\,, \qquad\qquad t(\bar{t}) \to b(\bar{b})l^\pm\,\nu. \tag{25}$$

which is clean for discovery.In addition to the backgrounds listed in equations 4-5, an additional background to be considered is

$$p\,p \;\;\to\;\; t\,W. \tag{26}$$

The single top SM background in equation 26 is irreducible.

4.3 Event Simulations for Heavy Bottom Quarks ($t + W +$ jet)

The basic selection cuts are all the same as for the W' boson search, up to the requirement

$$\not{E}_T > 25\ \text{GeV}. \tag{27}$$

In addition to these basic cuts, we now place additional cuts to optimize the signal.

From Fig. Ref.stopx:bprimekin, it is clear the p_T of leading jet for the signal is much larger than the backgrounds. We require

$$p_T \;\geq\; 80\ \text{GeV} \quad (\text{leading jet}) \tag{28}$$
$$p_T \;\geq\; 50\ \text{GeV} \quad (\text{subleading jet}). \tag{29}$$
$$p_T \;\geq\; 40\ \text{GeV} \quad (\text{additional jet}). \tag{30}$$

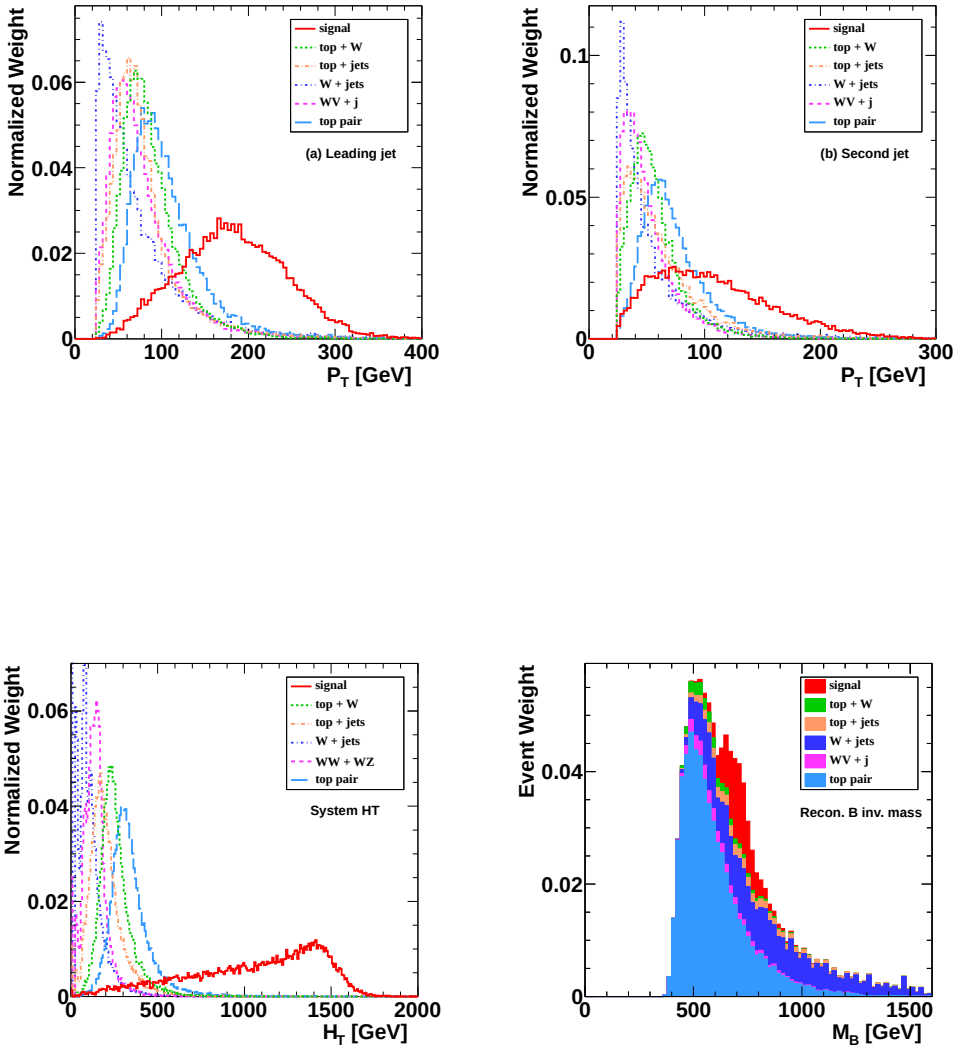

Figure 3: p_T distributions from the leading jet (upper right) and subleading jets (upper left). The H_T distribution is in the lower left panel. It is clear these variables can be used to separate the signal from the background. After the cuts, the reconstructed B' invariant mass distributions for signal and backgrounds is plotted in the lower right panel.

We again define the scalar sum of the p_T's of all the particles in the final state.

$$H_T = p_T^{\ell^+} + \not{E}_T + \sum_j p_T^j. \tag{31}$$

Here j runs over all of the well-separated jets in the event. We apply the following cut

$$H_T \geq 425 \text{ GeV}. \tag{32}$$

We impose the invariant mass window cuts

$$|m_{l\nu bjj} - m_{B'}| < 100 \text{ GeV}\,. \tag{33}$$

After these cuts, we show the B' resonance in Fig. Ref.stopx:bprimekin. For the heavy B' quark with 700 GeV mass, the significance with 1 fb$^{?1}$ luminosity is

$$S/\sqrt{B} \sim 6. \tag{34}$$

Cross sections for the various background processes without cuts are given in Table 2.

5 Conclusions

In this review, we focused on searches for new W' gauge bosons as well as B' heavy quarks. This is done under the rubric of searches for new physics under single top $+X$. A general survey of the possible new physics with associated single top production can be found in Ref. [401]. We showed TeV W' bosons and B' heavy quarks are easily accessible during the early LHC running.

Acknowledgements

We would like to thank S. Chivukula J. Hewett, T. Rizzo, E. Simmons and B. Shuve for useful discussions. The work of J.-H.Y. and C.-P. Y. is supported in part by the U.S. National Science Foundation under Grant No. PHY-0855561. This work of D.W. is supported in part by a grant from the National Academies of Science and the LHC Theory Initiative.

Appendix

A few basic definitions were used in the analysis in the previous sections are given here. We place some important definitions not included in the above text; if needed, see Ref. [432, 433] for additional background.

A Detector Effects

We often use b-tagging to increase the signal efficiency. A tagging efficiency of 60% is used in our analysis. We take into account a mis-tag rate for a light non-b quark (including the charm quark) to mimic a b jet, with mistag efficiency $\epsilon_{j\to b} = 0.5\%$

We smear the electron and hadronic energy according to Gaussians given by

$$\frac{\Delta E_j^e}{E_j^e} = \frac{0.05}{\sqrt{E_j/\text{GeV}}} \oplus 0.0055 \tag{A.1}$$

$$\frac{\Delta E_j^h}{E_j^h} = \frac{1}{\sqrt{E_j/\mathrm{GeV}}} \oplus 0.05, \tag{A.2}$$

respectively. The muon momentum is smeared by

$$\frac{\Delta p_T^l}{p_T^l} = 0.36\,\frac{p_T^l}{\mathrm{TeV}} \oplus \frac{0.013}{\sqrt{\sin\theta}}. \tag{A.3}$$

where θ is the polar angle of the lepton with respect to the beam direction in the lab frame. These smearing parameters are consistent with both the ATLAS and CMS experiments. Finally, we use FastJet to cluster the final state jets with a cone size $R = 0.4$.

B Top Tagging and Reconstruction

Hadronic Top Reconstruction: Here the top quark decays hadronically to a b-jet and a W bosons which subsequently decays to jets. In order to tag the top simply require the following invariant masses

$$m_W^2 = (p_1 + p_2)^2 \qquad\qquad m_t^2 = (p_1 + p_2 + p_3)^2. \tag{B.4}$$

to be within the ranges

$$77 < m_W < 83\ \ \mathrm{GeV} \qquad\qquad 168 < m_t < 176\ \ \mathrm{GeV}. \tag{B.5}$$

Semileptonic Top Reconstruction: For simplicity, we consider top decays to electrons or muons only. With only one neutrino in the final state, the missing momentum generates four unknowns. The missing transverse momentum

$$\not{\vec{p}}_T = -\sum_i \vec{p}_{T_i} \qquad\qquad \not{E}_T = -\sum_i E_i, \tag{B.6}$$

determines only two of the four components of the missing neutrino momentum. The rest of the components of the momentum can be determined by taking the W boson and top quark mass as an input for on-shell top quark production and decays. To see this explicitly, we first demand that $m_{l\nu}^2 = M_W^2$. The longitudinal momentum of the neutrino is formally expressed as

$$p_L^{(\nu)} = \frac{1}{2\,p_T^{(l)\,2}}\left(A\,p_L^{(l)} \pm E^{(l)}\sqrt{A^2 - 4\,p_T^{(l)\,2}\not{E}_T{}^2}\right), \tag{B.7}$$

where $A = M_W^2 + 2\,\vec{p}_T^{\,(l)} \cdot \not{\vec{E}}_T$. Again $l = e, \mu$. The two-fold degeneracy of the neutrino longitudinal momentum (above) is resolved by considering the top quark mass. Thus, if $A^2 - 4\,p_T^{(l)\,2}\,\not{E}_T{}^2 \geq 0$, the value of $p_{\nu L}$ that best yields the known top mass via $m_{l\nu b}^2 = m_t^2$ is selected.

Detector effects can reduce the top reconstruction efficiency and, in particular, force the radical in equation B.7 to be negative. In this case, in order to better recover the correct kinematics [432], we instead first reconstruct the top quark directly by demanding $m_{l\nu b}^2 = m_t^2$. The longitudinal momentum of the neutrino is expressed as

$$p_L^{(\nu)} = \frac{A'\,p_{(bl)\,L}}{2(E_{(bl)}^2 - p_{(bl)\,L}^2)} \tag{B.8}$$

$$\pm \quad \frac{1}{2(E^2_{(bl)} - p^2_{(bl)\,L})} \left(p^2_{(bl)\,L} A'^2 + (E^2_{(bl)} - p^2_{(bl)\,L})\,(A'^2 - 4E^2_{(bl)} \not{E}_T{}^2) \right)^{1/2}$$

where $A' = m_t^2 - M^2_{(bl)} + 2\,\vec{p}_{(bl)\,T} \cdot \vec{\not{E}}_T$ Here l runs over e, μ. The two-fold ambiguity is broken by choosing the value that best reconstructs $M_W^2 = m^2_{l\nu}$. Notice because $A' \sim m_t^2$ in the equation above, the value under the radical has a smaller chance of being negative.

C Spin Determination: Lepton Polarization

The charged lepton from top quark decay is maximally correlated with top quark spin. The connection between top quark spin and the charged lepton can be found from the distribution in $\theta_{\rm hel}$, the angle of the lepton in the rest frame of top quark relative to the topquark direction of motion in the overall c.m. frame. This is usually named as "helicity" basis. The angular correlation of the lepton ℓ^+ is given by

$$\frac{1}{\sigma}\frac{d\sigma}{d\cos\theta_{\rm hel}} = \frac{1 \pm \cos\theta_{\rm hel}}{2}, \tag{C.9}$$

with the $(+)$ choice for right-handed and $(-)$ for left-handed top quarks; Clearly, the charged lepton from a right-handed top quark prefers to move along the top quark direction . In the top-quark rest frame, 75% (25%) of charged leptons from t_R (t_L) decays follow the top-quark direction.